2003

† . 　 * . 　 * . 　 *

The Variation of Stress Concentration Factor and Crack Initiation Behavior on the Hole Defects Around the Rivet Hole in a Aircraft Materials

Sam-Hong Song, Cheol-Woong Kim, Tae-Soo Kim and Jin-Woo Hwang

Key Words : Rivet Hole(　　　), Hole Defect(　　　　), Hole Interaction(　　　　　　), Stress Concentration Factor(　　　　　), Crack Initiation Life(　　　　), Monolithic Aluminum(　　　　　　), Al/GFRP Laminates(　　/　　　　　　　), Multiple-Site Damage Crack(　　　　　　　, MSD)

Abstract

The material deficiencies in the form of pre-existing defects can initiated cracks and fractures. The stress distribution and fatigue crack initiation life of engineering materials may be associated with the size, the shape and the relative location of defects contained in the component. The objective of this study is to investigate the effect of arbitrarily located hole defect around the rivet hole of a wing section in monolithic aluminum and Al/GFRP laminates under cyclic bending moment during a service load. The stress distribution and the fatigue crack initiation behavior near a rivet hole of on the relationships between stress concentration factor (K_t) and relative position of defects were considered. The test results indicated the features of different stress field. Therefore, the stress concentration factor (K_t) and the fatigue crack initiation behavior was illustrated different behavior according to each position of hole defect around the rivet hole in monolithic aluminum and Al/GFRP laminates.

Al/GFRP

1.

．

(saw-cut) 　(circular hole) 　．

　．　Al/GFRP

，

/ 　Lawcock [1] 　CARALL

(Aluminum alloy/Glass Fiber Reinforced Plastic 　, 　Whitney 　Nuismer

Al/GFRP 　) 　(Average Stress Criterion, ASC)

，

． 　． Guo [2]

．

†　　　　　　，　　，
E-mail : shsong@korea.ac.kr
TEL : (02)3290-3353　FAX : (02)921-8532
*　　　　，

ARALL

(prepreg)

Al/AFRP ,[3]

Al/AFRP

[4,5] .

,

.

.

,

.

(K_t),

Al/GFRP

.

(K_t)

.

2.

2.1

Al/GFRP

Al5052 (S-glass)

1/2([Al/GFRP/Al])

. Al5052

Table 1 Table 2 .

-

(post-heating)

(DSC)

2.2

Al/GFRP Fig. 1

5mm

.

Fig. 1 B

,

Fig. 2 (a)

4

. x θ_1 = 0°,

θ_2 = 30°, θ_3 = 60°, θ_4 = 90°

0.5mm, 0.5mm

. Murakami[6]

(2L) $2L \leq 2a_1 + a_2$

.

( ) 2mm .

Fig. 2 (b) a_1 = 2.5mm, a_2 = 0.25mm

Murakami

2L = 5.25 mm 2L = 4.75mm

.

(Al5052) Al/GFRP

Al/GFRP

.

Table 1 Mechanical properties of Al5052

Alloy	Tensile strength (MPa)	Yielding strength (0.2% offset) (MPa)	Thickness (mm)
Al5052	283	228	0.5

Table 2 Mechanical properties of S-glass fiber

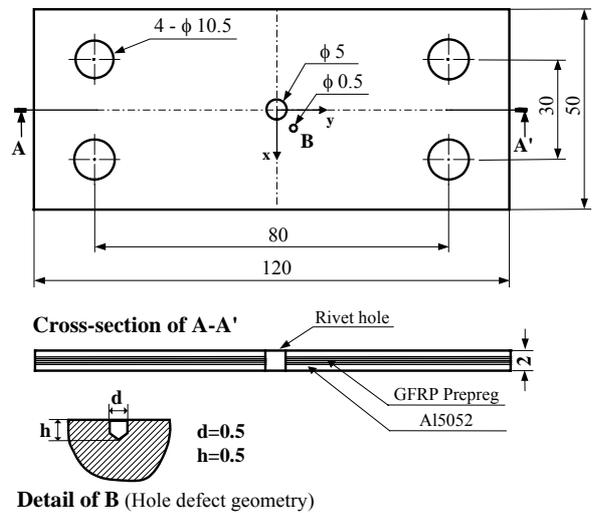| Fiber type	Ultimate tensile strength (MPa)	Tensile modulus (GPa)	Tensile strain to failure (%)	Density (g/cm³)
S-glass	4600	86	5.3	2.6

Fig. 1 Geometries of specimen (unit : mm)

2.3

(TB-10B, Shimadzu Co.) .

98 N-m , 2000 rpm, 33.3 Hz .

Al/GFRP -

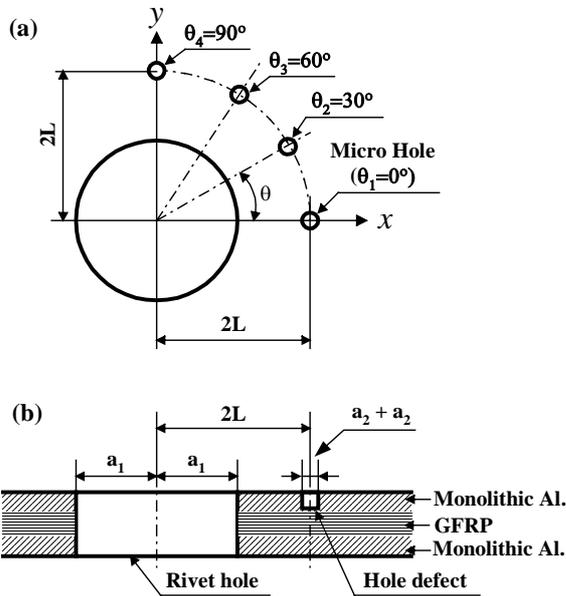.   ,

(7)

.

R = -1

. , Al/GFRP

$$\sigma_{max} = 120 \text{ MPa}$$.

100

.

3.

3.1   (K$_t$)

.

Al/GFRP

.

3.1.1   (Al5052)

(K$_t$)

Fig. 4 (a),

(b), (c), (d)   θ = 0°, θ =

30°, θ = 60°, θ = 90°

.   ANSYS

4940   , 1600   shell

.   (K$_t$)

(1)   .

$$K_t = \frac{\sigma_{max}}{\sigma_{nom}} \tag{1}$$

(a)

Fig. 2 Relationship position between rivet hole and hole defects
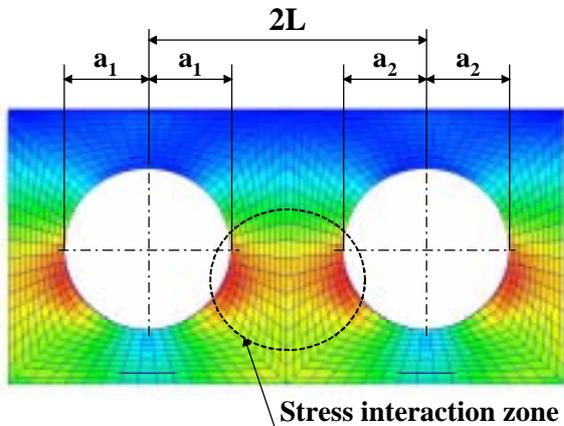

Stress interaction zone

Fig. 3 Relationship position of two hole and stress interaction zone (the distance between two hole(2L) should be less than $2a_1 + a_2$ to observe stress interaction)

(a) θ = 0º   **(b) θ = 30º**

(c) θ = 60º   **(d) θ = 90º**

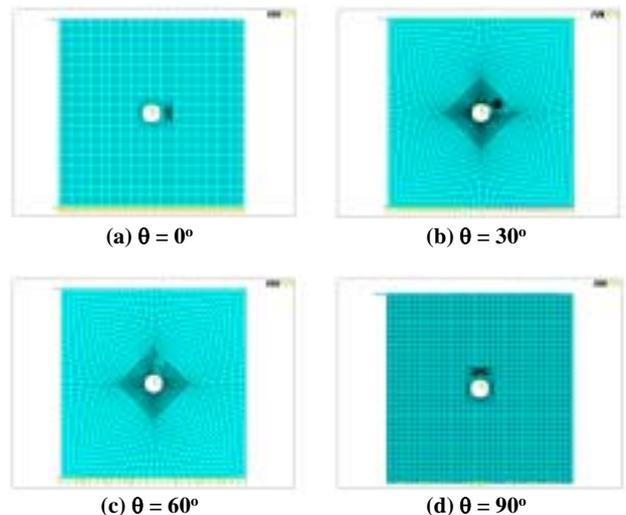**Fig. 4** FE model on the variable hole defects around the rivet hole

, σ_{max}

, σ_{nom} .

                                                        Fig.

5   .

                                        .

                                                    K_t =1.73

                        $\theta = 0°$ K_t =3.23, θ =

30° K_t =2.98, $\theta = 60°$ K_t =2.18, $\theta = 90°$

      K_t =1.79   .

        $\theta = 0°$ $\theta = 90°$

                                    .   , $\theta = 60°$

                                          .

      $\theta = 60°$,

                              .   ,

                  $\theta = 30°$ $\theta = 60°$

              .   ,

      (K_t)

                                    Fig. 6

          . Fig. 6   (2)

          (equivalent stress)   Von mises

              .

$$\sigma_{eq} = \frac{1}{\sqrt{2}}\left[(\sigma_1 - \sigma_2)^2 + (\sigma_2 - \sigma_3)^2 + (\sigma_3 - \sigma_1)^2\right]^{\frac{1}{2}} \qquad (2)$$

σ_{eq} . Fig. 6

                              , Fig. 6 (a)

                                        ,

                  .   , Fig. 6 (b),(c) $\theta = 0°$ θ

= 30°

                                        .

                                    ,

                                                        .

        , $\theta = 60°$ $\theta = 90°$

                                                        .

                                            $\theta = 60°$, $\theta = 90°$

      Murakami

                                        ,

                  ,

                                        .

(a) *without* hole defect

(b) hole defect ($\theta = 0°$)   (c) hole defect ($\theta = 30°$)

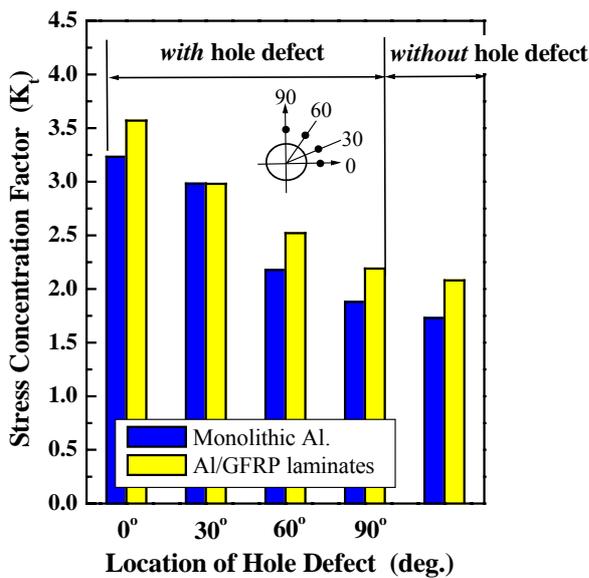(d) hole defect ($\theta = 60°$)   (e) hole defect ($\theta = 90°$)

Fig. 5 Stress concentration factor on the relative position of hole defect in *monolithic aluminum* versus *Al/GFRP laminates*
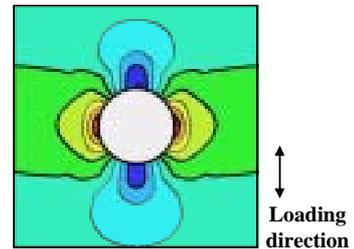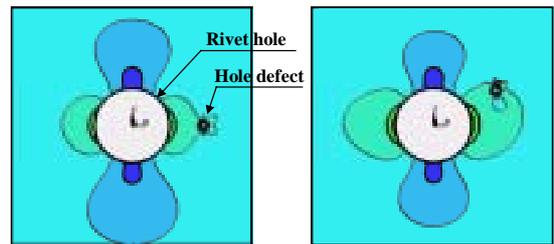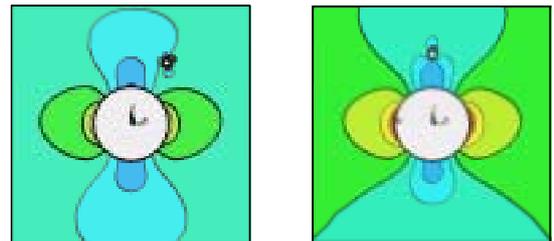
Fig. 6 Von mises stress distribution on the interaction between rivet hole and hole defect in *monolithic aluminum*

3.1.2 Al/GFRP
Al/GFRP

$\theta = 0°$, $\theta = 30°$, $\theta = 60°$ $\theta = 90°$

.

8-node,

shell 99(liner layer)
.
Fig.

5   . Al/GFRP

,

K_t =2.08 $\theta = 0°$ K_t
=3.57, $\theta = 30°$ K_t =2.98, $\theta = 60°$ K_t =2.52,
$\theta = 90°$ K_t =2.19   .
$\theta = 0°$

$\theta = 90°$

. Fig. 5

Al/GFRP

,   Al/GFRP

15%   .

Al/GFRP

,   2   .

,

.   . , Al/GFRP

Al/GFRP

. Al/GFRP

.

,

.

Al/GFRP

. , Fig. 7

4   Al/GFRP

,

Fig. 7 (a)

Al/GFRP

Fig. 7 (b)

.

Al/GFRP

. Fig.

8

.

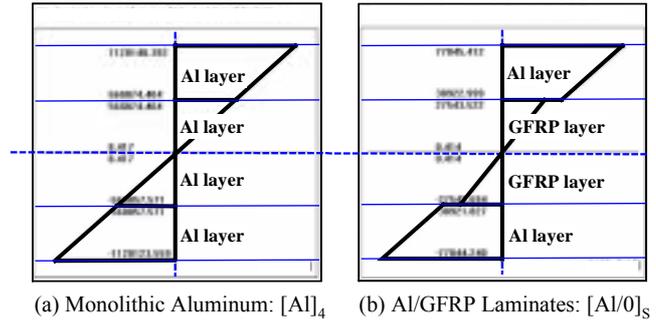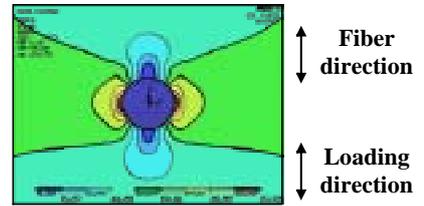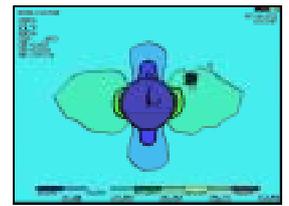(a) Monolithic Aluminum: [Al]₄   (b) Al/GFRP Laminates: [Al/0]ₛ

Fig. 7 The result of interlaminar stress distribution on the (a) monolithic aluminum : [Al]₄, (b) Al/GFRP laminates : [Al/0]ₛ

(a) *without* **hole defect**
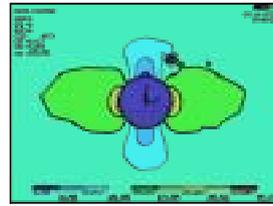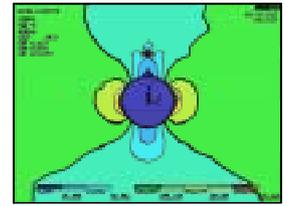

(b) hole defect ($\theta = 0°$)   **(c) hole defect ($\theta = 30°$)**

(d) hole defect ($\theta = 60°$)   **(e) hole defect ($\theta = 90°$)**

Fig. 8 Von mises stress distribution on the interaction between rivet hole and hole defect in *Al/GFRP laminates*

Von mises

.

, $\theta =$
0°, $\theta = 30°$

Al/GFRP $\theta = 0°$, $\theta =$
30°, $\theta = 60°$

.   Al/GFRP

. ,

$\theta = 60°$

.

2003

Al/GFRP　　　　　　　　3.2.1

，

. Manson[9]

1/10

3.2

，braglia　　[10]

－　　　　　　　Al/GFRP

0.25mm　　　　　　　　　　　　　　　　.

4　　　　　　.[8]　　　Al/GFRP

，　　　　　　　　　　　　　　　　　　2mm　　　　　　　　　　2mm

(K)　　　　　　　　(COD)　　　　　　　　.

，

.　　　　　　　　　　　　，

(N_i)　　　　　　. Fig. 9 (a)

.
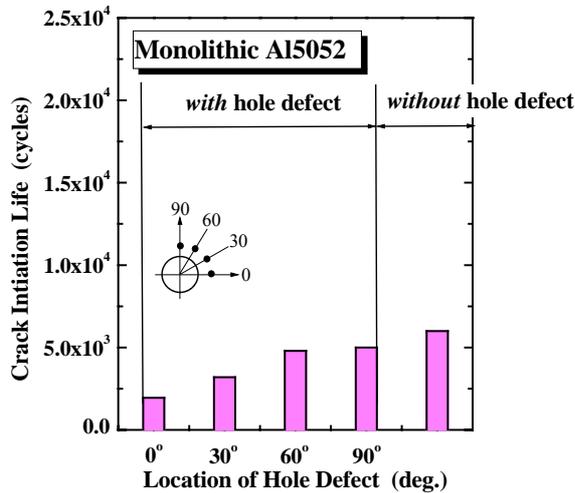
(a) In case of monolithic aluminum

(N_i)　　N_i = 6.0×10^3 cycles　　　，
(N_f)　　N_f = 1.7×10^4 cycles　　.
$\theta = 0°$
$\theta = 30°$, $\theta = 60°$, $\theta = 90°$

.

，

$\theta = 0°$, $\theta = 30°$

. $\theta = 0°$　　　68%
, $\theta = 30°$　　　47%　　　　　, $\theta = 60°$　　20%　　　　　, $\theta = 90°$　　　17%
. Fig. 5
$\theta = 0°$, $\theta = 30°$
$K_t = 3.1$　　　　, $\theta = 60°$, $\theta = 90°$
$K_t = 2.0$

.

.

3.2.2 Al/GFRP

Al/GFRP

.　　　　　　　　　　　　，

，　　　　　　，　　　　　　，

.
[4,5,8,11]
.

Al/GFRP　　　　　　　　(　　　　　)

. Al/GFRP

(N_i)

. Fig. 9 (b)　　Al/GFRP

.
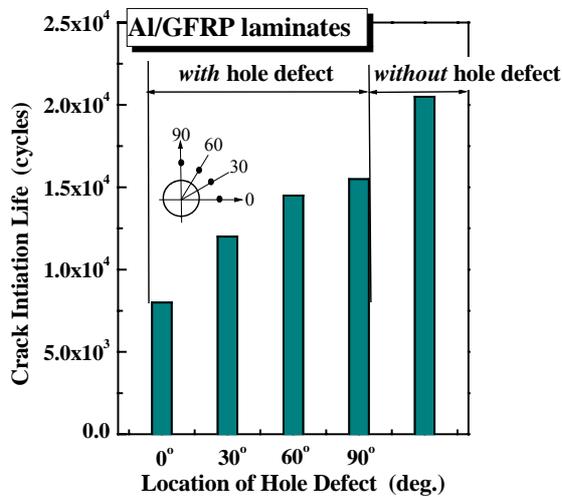
(b) In case of Al/GFRP laminates

Fig. 9 Crack initiation life in case of variable hole defects

(N_i) $N_i =$ Partl [12]   , MSD

2.1×10^4 cycles (N_f) $N_f =$,

9.2×10^4 cycles   . Al/GFRP

4   20%

. $\theta = 0°$ $\theta =$.

$30°, \theta = 60°, \theta = 90°$ MSD

. , $\theta = 0°$ $\theta = 30°$

. ,   Al/GFRP

, Al/GFRP $\theta = 0°$ $\theta = 30°$

MSD .

. , $\theta = 0°$ $\theta = 30°$,

.   Fig. 5   ,

$\theta = 0°$ $\theta = 30°$

.   Fig. 9   .

Fig. 10 $\theta = 0°$ $\theta = 30°$

. Fig. 9   .   ,

$\theta = 0°$ Al/GFRP

. , Al/GFRP   ,   MSD

Al/GFRP

. , $\theta = 0°$

$\theta = 30°$,   MSD

Fig. 10 $\theta = 0°$. ,

Al/GFRP   ,

, $\theta = 30°$

Al/GFRP   .

. $\theta = 30°$

MSD(Multiple-Site Damage)   .   4.

,

,

.

.

Fig. 10 Crack profile at $\theta = 0°$ and $\theta = 30°$ in *monolithic aluminum* and *Al/GFRP laminates*

(1)

.

i)   ,

$\theta = 0°$ $\theta = 90°$

. , $\theta = 0°$ $\theta = 30°$

, $\theta = 60°$

. , $\theta = 0°$ $\theta = 30°$

.

ii) Al/GFRP   ,

$\theta = 0°$ $\theta = 90°$

,

2003

15% . , Al/GFRP

, , Al/GFRP

.

(2)

i) ,
θ = 0° θ = 90°
. , θ = 0° , θ = 30° θ
= 60°, θ = 90°
, θ = 0°, θ = 30° θ
= 60°, θ = 90°

.

ii) Al/GFRP ,
4 .
θ = 0° θ = 90°

. , Al/GFRP

,

.

. , θ = 30°

MSD

, Al/GFRP

. ,

.

Mixture Ratio Effect of Epoxy Resin, Curing Agent and Accelerator on the Fatigue Behavior of FRMLs," *Transactions of the KSME, A*, Vol. 25, No. 4, pp. 592~601.

(4) Sam-Hong Song and Cheol-Woong Kim, 2001, "The Delamination and Fatigue Crack Propagation Behavior in Al5052/AFRP Laminates Under Cyclic Bending Moment," *Transactions of the KSME, A*, Vol. 25, No. 8, pp. 1277~1286.

(5) Sam-Hong Song and Cheol-Woong Kim, 2003, "Fatigue Crack and Delamination Behavior in the Composite Material Containing a Saw-cut and Circular Hole (I) -Aramid Fiber Reinforced Metal Laminates-," *Transactions of the KSME, A*, Vol. 27, No. 1, pp. 58~65.

(6) Y. Murakami and S. Nemat-Nasser, 1982, "Interaction Dissimilar Semi-Elliptical Surface Flaws Under Tension and Bending," *Engineering Fracture Mechanics*, Vol. 16, pp. 373~386.

(7) Jan Willem Gunnink, 1990, "Aerospace ARALL the Advancement in Aircraft Materials," *35th International SAMPE Symposium*, pp. 1708~1721.

(8) Sam-Hong Song and Cheol-Woong Kim, 2003, "The Fatigue Crack and Delamination Behavior on the Fuselage-wing Intersection Containing Variable Notches," *International Journal of Modern Physics B*, Vol. 17, Nos. 1 & 2, pp. 401~406.

(9) S. S. Manson, 1953, "Behavior of Materials Under Conditions of Thermal Stress," *Heat Transfer Symposium*, Univ. of Michigan Engineering Research Institute, pp. 69~75.

(10) B. L. Braglia and R. W. Hertzberg, 1979, "Crack Initiation in a High Strength Low-Alloy Steel," *Fracture Mechanics*, ASTM STP 677.

(11) Sam-Hong Song and Cheol-Woong Kim, 2003, "The Analysis of Fatigue Behavior Using the Delamination Growth Rate(dA_D/da) and Fiber Bridging Effect Factor(F_{BE}) in Al/GFRP Laminates," *Transactions of the KSME, A*, Vol. 27, No. 2, pp. 317~326.

(12) O. Partl and J. Schijve, 1993, "Multiple-Site Damage in 2024-T3 Alloy Sheet," *International Journal of Fatigue*, Vol. 15, No. 4, pp. 293~299.

(1) G. Lawcock, L. Ye and Y. W. Mai, 1997, "Progressive Damage and Residual Strength of a Carbon Fiber Reinforced Metal Laminates," *Journal of Composite Materials*, Vol. 31, No. 8, pp. 762~787.

(2) Y. Guo and X. Wu, 1999, "Bridging Stress Distribution in Center-Cracked Fiber Reinforced Metal Laminates : Modeling and Experiment," *Engineering Fracture Mechanics*, Vol. 63, pp. 147~163.

(3) Sam-Hong Song and Cheol-Woong Kim, 2001, "The